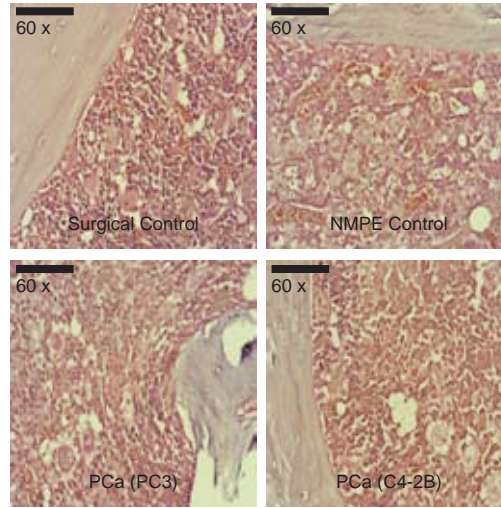
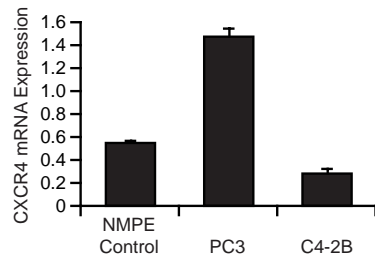


A.



B.



C.

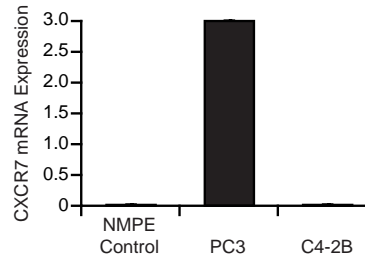


**Figure S1: The marrow histology of PCa-bearing mice and PCa gene expression, related to Figure 1.**

(A) The representative H&E images of bone marrow histology of the mice that had developed metastases at 16 weeks (See also Figure 1D). Original magnification 60 x. Bar = 50 µm. (B&C) mRNA levels of (A) CXCR4 and (B) CXCR7 in PCa cultured in vitro. Presented as mean ± s.e.m.

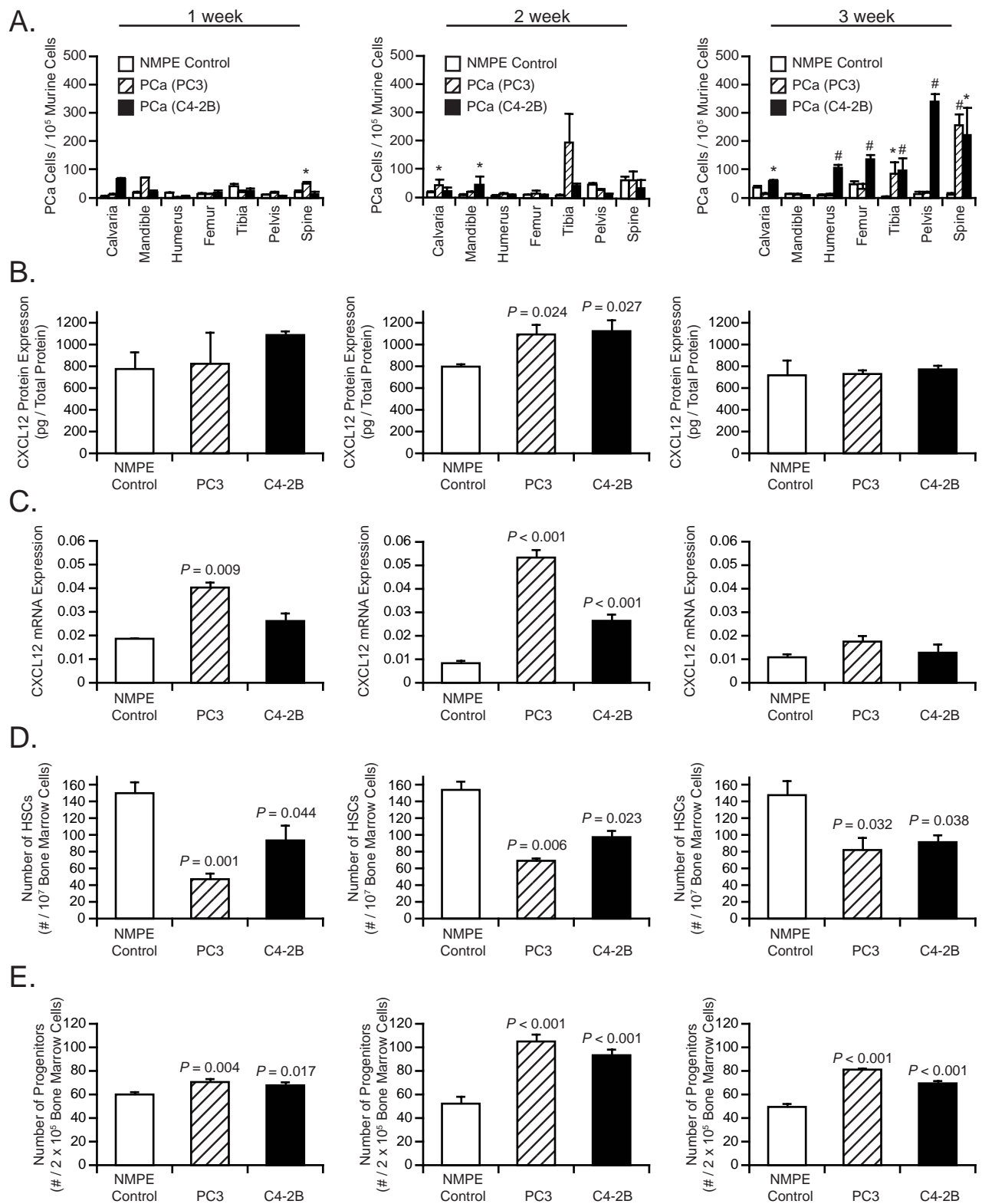


**Figure S2: The temporal relationship between disseminated PCa, hematopoietic stem and progenitors, and CXCL12 levels in marrow during metastasis.**

SCID mice were implanted either NMPE cells or PCa (PC3 or C4-2B). Animals were sacrificed weekly (n = 5 per group), and the bone tissues and the bone marrow cells were collected. **(A)** The number of metastatic cells was determined by QPCR. Presented as mean  $\pm$  s.e.m., \**p* < 0.05 and #*p* < 0.01 versus NMPE control group (Kruskal-Wallis test). **(B&C)** The levels of CXCL12 in the marrow were measured by **(B)** QRT-PCR (mean  $\pm$  s.e.m., significant differences from the NMPE control group, Kruskal-Wallis test) and by **(C)** ELISA (mean  $\pm$  s.e.m., significant differences from the NMPE control group, Student's *t* test). **(D)** The numbers of HSCs (Lin-CD150+CD41-CD48-Sca-1+cKit+cells) in the marrow (from femur and tibia) were enumerated by FACS and **(E)** hematopoietic progenitor numbers (from femur and tibia) were determined using colony-forming assays. Presented as mean  $\pm$  s.e.m., significant differences from the NMPE control group (Student's *t* test).

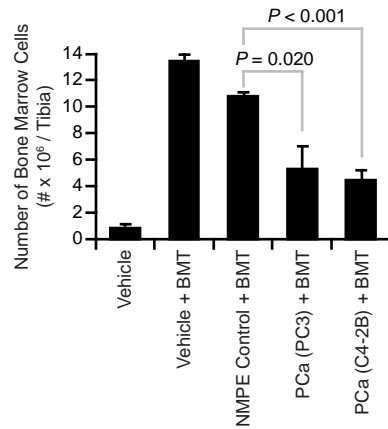
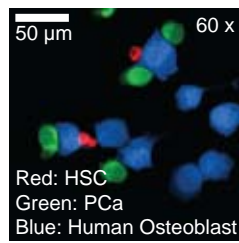


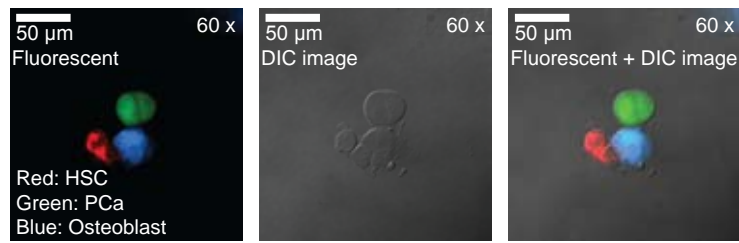
**Figure S3: Disseminated PCa prevent HSC engraftment to the bone marrow, related to Figure 2.**

BMT were performed in the presence or absence of PCa cells (PC3 or C4-2B) or NMPE control cells. The numbers of bone marrow cells were counted following competitive BMT of animals presented in (Figure 2C). Presented as mean  $\pm$  s.e.m., significant differences from the NMPE control group (Student's *t* test).

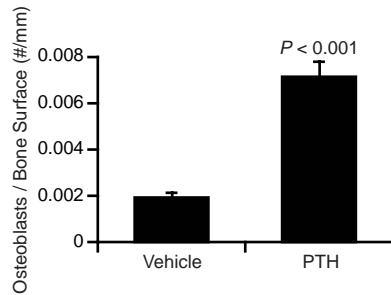
A.



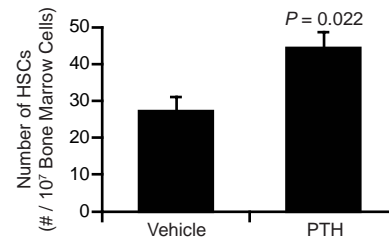
B.



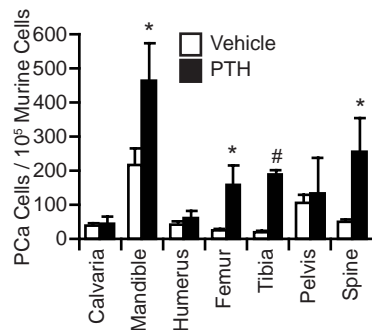
C.



D.



E.



F.

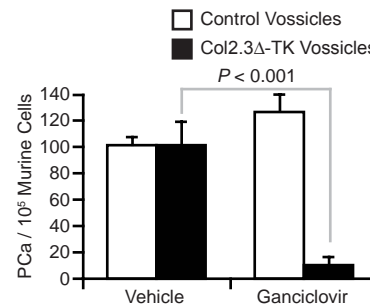


**Figure S4: HSC and PCa co-localize to marrow niches and alteration of niche size regulates tumor dissemination, related to Figure 4.**

(A&B) HSCs (Lin-CD150+CD41-CD48-Sca-1+cKit+cells) and PCa co-localize to (A) a single human osteoblast and (B) murine osteoblast with the differential interference contract (DIC) image in vitro (See also Figure 4B). Bar = 50 μm. (C-F) Alteration of niche size regulates disseminated of the PCa cell line C4-2B (See also Figure 4F&G). (C) Osteoblast numbers after PTH treatments were determined in the long bones and (D) the numbers of HSCs in the marrow after PTH treatments were counted by FACS. The data are presented as mean ± s.e.m., significant differences from the vehicle treatment (Student's *t* test). (E) Animals were pretreated with PTH or vehicle prior to establishing C4-2B s.c. tumors and the number of disseminated cells was determined at 3 weeks (n = 8 per group). Presented as the mean ± s.e.m. \**p* < 0.05 and #*p* < 0.01 versus vehicle treatment (Kruskal-Wallis test). (F) Comparison of homing of PCa (C4-2B) to Col2.3Δ-TK versus control vossicles with or without ganciclovir (n = 8 per group). The control vossicle with vehicle treatment were set as 100%. Presented as the mean ± s.e.m., significant differences from the Col2.3Δ-TK vossicle with vehicle treatment (Kruskal-Wallis test).

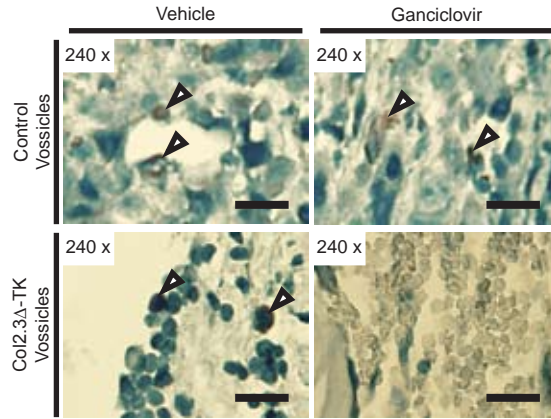


**Figure S5: The osteoblastic niche is critical for PCa growth in bone, related to Figure 5.**

Luciferase labeled PC3 (**PC3<sub>luc</sub>**) were placed directly into Col2.3 $\Delta$ -TK or control vossicles which were subsequently implanted into the immunodeficient mice. Mice were treated with either ganciclovir or vehicle for 3 weeks to ablate the osteoblast niche. Cytokeratin-immunostained vossicles. High magnification images of Figure 5B. Arrow heads: cytokeratin positive cells. Bar = 50  $\mu$ m.

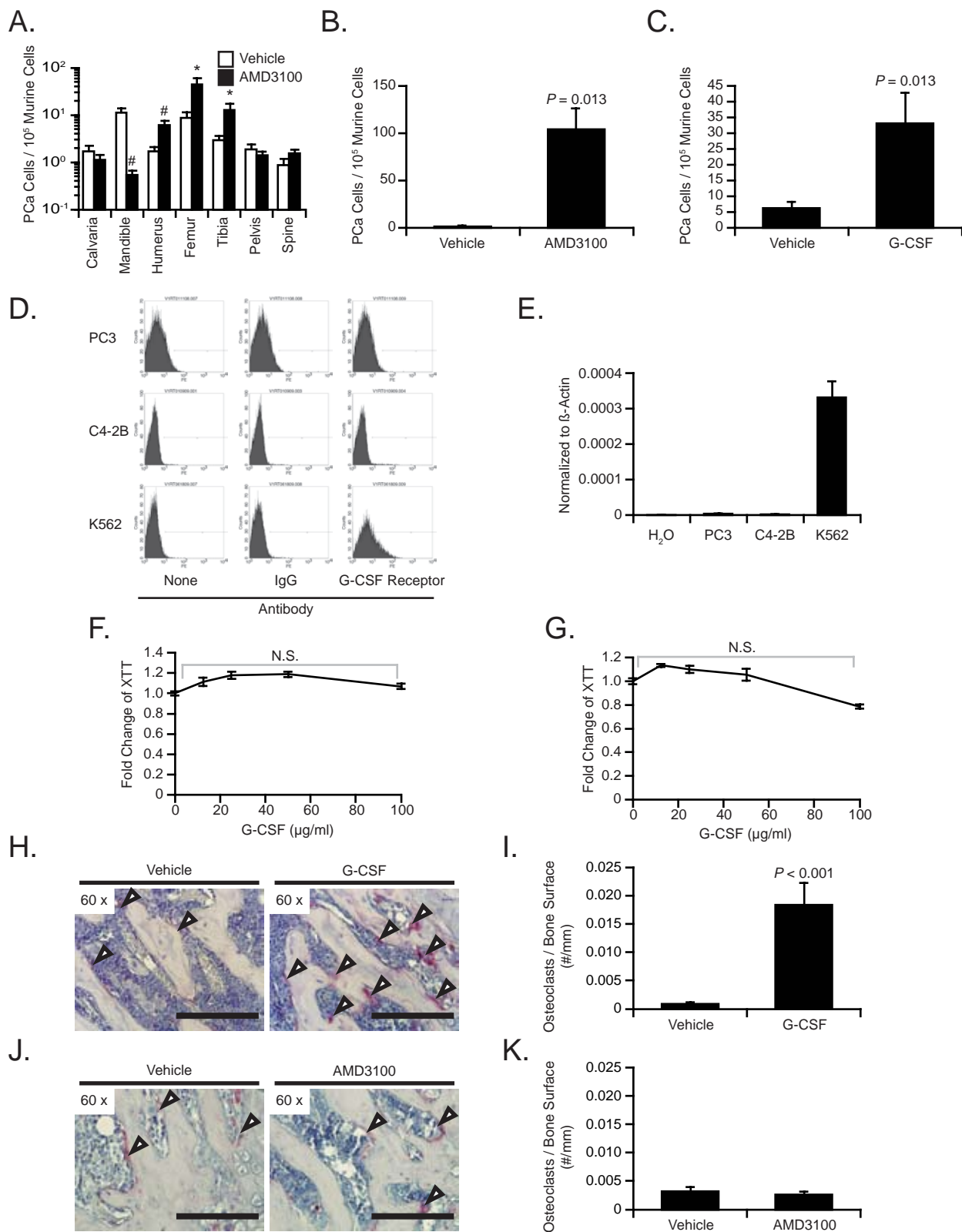
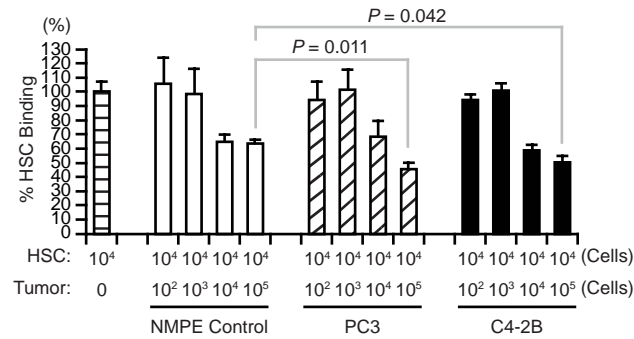


**Figure S6: PCa target HSC niche and AMD3100 and G-CSF mobilize metastatic PCa from the bone marrow, related to Figure 6.**

(A) C4-2B cells target to the HSC niche (See also Figure 6A&B). The numbers of PCa cells in the marrow were assessed by QPCR. \* $p < 0.05$  and # $p < 0.01$  versus vehicle (Kruskal-Wallis test). (B) Peripheral blood levels of PCa (C4-2B) cells mobilized with AMD3100 or vehicle evaluated by QPCR (See also Figure 6C&D). Significant differences from vehicle treatment groups (Kruskal-Wallis test). (C) Peripheral blood levels of PCa (C4-2B) cells mobilized with G-CSF or vehicle evaluated by QPCR (See also Figure 6H). Significant differences from the vehicle treatment group (Kruskal-Wallis test). (D) PCa cells (PC3 and C4-2B) express low/no levels of G-CSF receptors by FACS. K562 (a bcr/abl positive erythroleukemia line) served as a positive control. (E) Representative QRT-PCR analysis of G-CSF receptor expression by PCa (PC3 or C4-2B). Presented as the mean  $\pm$  s.e.m. H<sub>2</sub>O served as negative controls and K562 cells (a bcr/abl positive erythroleukemia line) served as positive controls for G-CSF receptor. (F&G) G-CSF does not stimulate (F) PC3 and (G) C4-2B proliferation over a 3 day period (XTT assay; mean  $\pm$  s.e.m.). (H-K) Representative TRAP staining of the long bones of (H) G-CSF and (J) AMD3100 treated animals. (I&K) Osteoclasts numbers were quantified on the long bone sections. Original magnification at 60 x. Bar = 50  $\mu$ m.

A.



B.

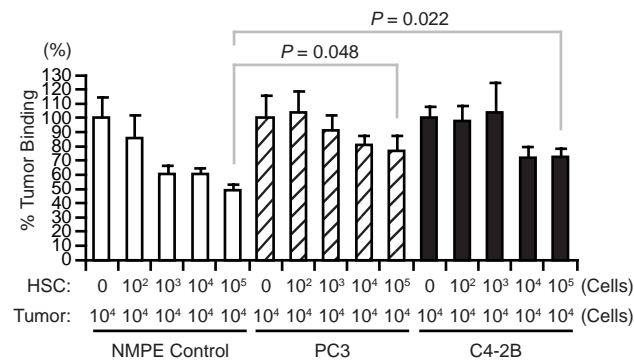


**Figure S7: Molecular mechanisms regulating niche competition between PCa and HSCs - competition for binding to osteoblasts, related to Figure 7.**

(A) Competition binding assays to Anxa2 peptide between HSC (Lin-Sca-1+cKit+ cells) (104 cells) and PCa cells or NMPE control cells (0-105 cells) (See also Figure 7A). Data are presented as the mean  $\pm$  s.e.m. Significant differences from controls (Student's *t* test). (B) A fixed number of labeled NMPE control cells and PCa cells (104 cells) and different numbers of HSC (0-105 cells) were layered onto Anxa2 peptide. The binding ability of NMPE control cells and PCa cells to Anxa2 peptide in presence of HSCs was evaluated using a fluorescent plate reader (See also Figure 7G). Data are presented as the mean  $\pm$  s.e.m. Significant differences from controls (Student's *t* test).

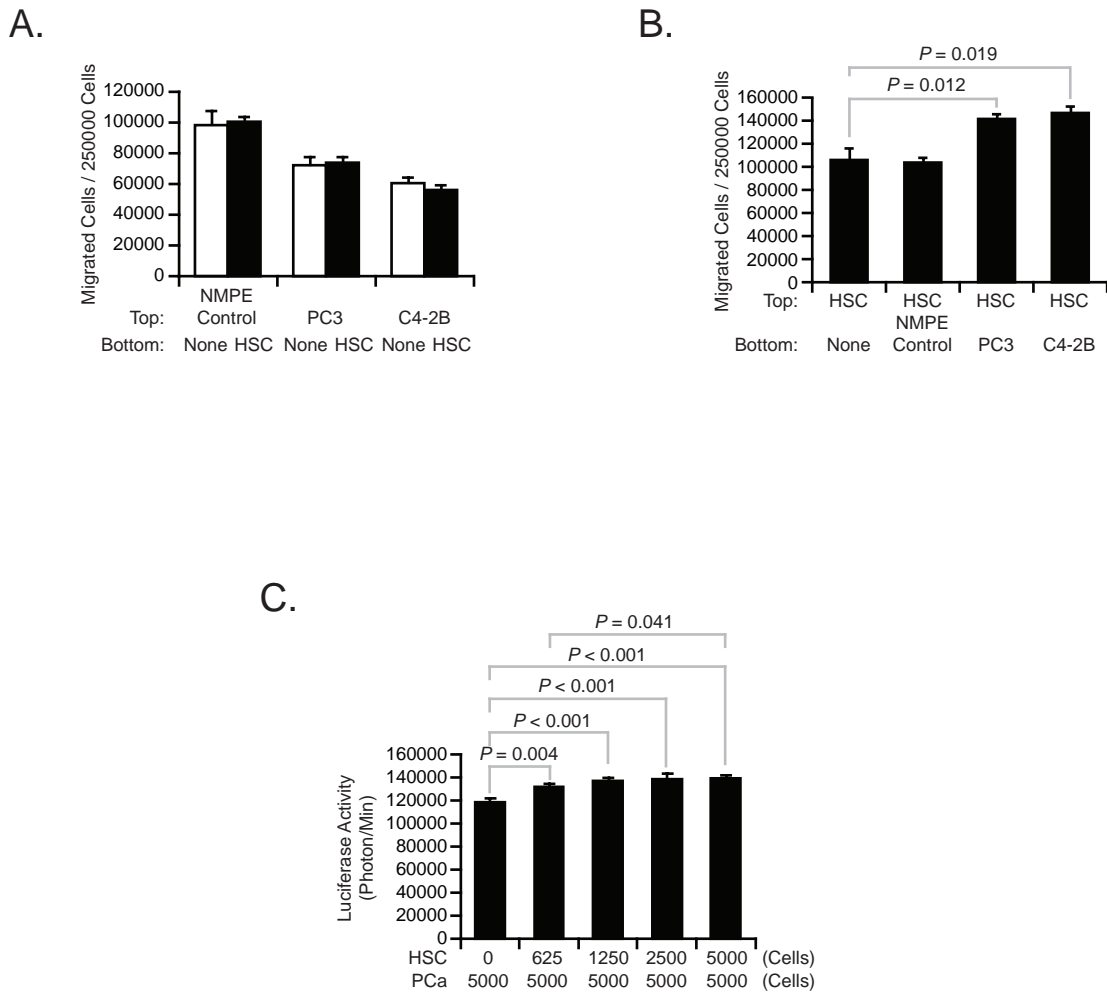


**Figure S8: Direct interaction between PCa and HSCs.**

(A) PCa migration toward HSCs (Lin-Sca-1+cKit+ cells) and (B) HSC (Lin-Sca-1+cKit+ cells) migration toward PCa. Presented as the mean  $\pm$  s.e.m. (Student's *t* test). (C) Luciferase labeled PCa cells were grown in the presence/absence of HSC (Lin-Sca-1+cKit+ cells), where luciferase activity was evaluated as a reflection of cell growth. Presented as the mean  $\pm$  s.e.m. (Student's *t* test).

## **Supplemental Methods and Notes:**

### **An *in vivo* animal model for solid tumor metastasis**

We recently developed the *in vivo* model to track early disseminated event of solid tumor by a sensitive real-time polymerase chain reaction (**QPCR**) assay using a human specific ALU sequence (1). In this model, human prostate cancer (**PCa**) cell lines are implanted in sterile collagen scaffolds into immunodeficient mice subcutaneously or orthotopically (prostate) as models of primary tumors. At various time points, the animals can be sacrificed, and various tissues may be collected to extract DNA. Using **QPCR**, the disseminated tumor cells shed from cells within the collagen scaffolds (or primary tumors) can be evaluated. At 3 weeks, several PCa cell lines (PC3 and C4-2B) are able to spread from the primary tumor and take up residence in distant sites.

This model allows us to study the disseminated tumor cells from a primary site. To do this, PCa cells are implanted as a 'primary tumor' into animals subcutaneously. After 3 weeks, the tumors are removed. If the luciferase-labeled PCa cells are utilized, in several cases, metastatic lesions are identified by bioluminescence imaging (**BLI**) at 9 months (SCID mice) and at 3 months (NOD/SCID mice (manuscript in preparation)).

Another innovative aspect of this model is the ability to incorporate genetic/transgenic approaches into tumor studies without extensive back crossing of animal models. By transplanting target tissues (e.g. vertebral bodies, or vessicles from both wild-type animals and gene knock out animals) into the host animals, we are able to explore the microenvironmental functions within a same animal (2).

By manipulating the microenvironment (e.g. neutralizing adhesion molecules, altering chemokine concentration gradients, or increasing endocrine hormones), this novel *in vivo* model provides us opportunities to explore the molecular mechanisms in the early tumor dissemination and identify the metastatic niche.

### **Non-metastatic prostate epithelial cell lines**

Normal human prostate cells were obtained from patients undergoing prostatectomy in accordance with the University of Michigan's Investigation Review Board. The tissue was collected from a distal location from the tumor (within the prostate). The cells were passaged serially until stable cell lines were established. These cells are morphologically and pathologically distinct from the tumor.

### **Disseminated PCa utilize CXCL12 to compete HSC niche with HSCs**

To determine the temporal relationship between PCa micrometastases, CXCL12 levels and hematopoietic stem and progenitor numbers in the bone marrow of mice implanted with *s.c.* tumors over time were examined. Few if any PCa cells were identified in marrow after one week. The number of disseminated PCa cells began to rise as early as 2 weeks, such that by 3 weeks the numbers of tumor cells in marrow were significantly elevated (**Fig. S2, A**). In contrast, changes in marrow levels of CXCL12 mRNA levels were noted as early as 1 week after *s.c.* tumor implantation, with CXCL12 protein levels increasing at 2 weeks (**Fig. S2, B&C**). By 3 weeks CXCL12 mRNA and protein levels had returned to baseline levels (**Fig. S2, B&C**). FACS analysis showed that as early as 1

week HSC cells in marrow had decreased while progenitor cell populations expanded and alteration of these levels were maintained over the course of the studies (**Fig. S2, D&E**).

### **Annexin II Deficient animals**

Previous work has demonstrated that annexin II (**Anxa2**) is a surface protein which stimulates tissue plasminogen activator-mediated plasminogen activation. Anxa2-deficient animals displayed deposition of fibrin in the microvasculature and markedly diminished neovascularization of fibroblast (3).

Multiple cell-cell interactions play a crucial role in the development of hematopoietic stem cell (**HSC**) homing and solid tumor metastasis to the bone marrow. We recently observed that Anxa2 is highly expressed osteoblasts and endothelial cells in the bone marrow (4), and that anxa2 is involved in HSC homing (4) and prostate cancer (**PCa**) to the bone marrow (2). Adhesion of HSCs and PCa to osteoblasts derived from Anxa2-deficient animals is significantly impaired compared with osteoblast obtained from wild-type animals (2, 4). Most importantly, fewer HSCs are found in the marrow of Anxa2-deficient animals, compared to wild-type animals (4). Along with these findings, engraftment of HSC and localization of PCa into the bone marrow is substantially inhibited by blocking Anxa2 or its receptor in animal models (2, 4).

These data suggest that Anxa2 expressed by osteoblasts and endothelial cells plays a critical role in niche selection of both HSC and PCa.

### **Col2.3Δ-TK transgenic animals**

A transgenic mouse line was generated by bearing a fusion gene composed of the 2.3-kb fragment of the rat type I collagen  $\alpha 1$  (**Col1  $\alpha 1$** ) promoter and the herpes thymidine kinase gene (**HSV-TK**) (5). This transgenic mouse line was named as Col2.3Δ-TK animals. Col1  $\alpha 1$  expression is largely restricted to differentiated osteoblasts. When mice are treated with ganciclovir (**GCV**), the bone lining cells, osteoblasts, and bone marrow cellularity are reduced (5-7).

## Reference Lists

1. Havens, A.M., Pedersen, E.A., Shiozawa, Y., Ying, C., Jung, Y., Sun, Y., Neeley, C., Wang, J., Mehra, R., Keller, E.T., et al. 2008. An in vivo mouse model for human prostate cancer metastasis. *Neoplasia* 10:371-380.
2. Shiozawa, Y., Havens, A.M., Jung, Y., Ziegler, A.M., Pedersen, E.A., Wang, J., Lu, G., Roodman, G.D., Loberg, R.D., Pienta, K.J., et al. 2008. Annexin II/annexin II receptor axis regulates adhesion, migration, homing, and growth of prostate cancer. *J Cell Biochem* 105:370-380.
3. Ling, Q., Jacovina, A.T., Deora, A., Febbraio, M., Simantov, R., Silverstein, R.L., Hempstead, B., Mark, W.H., and Hajjar, K.A. 2004. Annexin II regulates fibrin homeostasis and neoangiogenesis in vivo. *J Clin Invest* 113:38-48.
4. Jung, Y., Wang, J., Song, J., Shiozawa, Y., Havens, A., Wang, Z., Sun, Y.X., Emerson, S.G., Krebsbach, P.H., and Taichman, R.S. 2007. Annexin II expressed by osteoblasts and endothelial cells regulates stem cell adhesion, homing, and engraftment following transplantation. *Blood* 110:82-90.
5. Visnjic, D., Kalajzic, I., Gronowicz, G., Aguila, H.L., Clark, S.H., Lichtler, A.C., and Rowe, D.W. 2001. Conditional ablation of the osteoblast lineage in Col2.3deltatk transgenic mice. *J Bone Miner Res* 16:2222-2231.
6. Visnjic, D., Kalajzic, Z., Rowe, D.W., Katavic, V., Lorenzo, J., and Aguila, H.L. 2004. Hematopoiesis is severely altered in mice with an induced osteoblast deficiency. *Blood* 103:3258-3264.

7. Zhu, J., Garrett, R., Jung, Y., Zhang, Y., Kim, N., Wang, J., Joe, G.J., Hexner, E., Choi, Y., Taichman, R.S., et al. 2007. Osteoblasts support B-lymphocyte commitment and differentiation from hematopoietic stem cells. *Blood* 109:3706-3712.